14th International Conference on Applications of Statistics and Probability in Civil Engineering, ICASP14
Dublin, Ireland, July 9-13, 2023

Physics model-based probabilistic process optimization and control

Paromita Nath
Assistant Professor, Department of Mechanical Engineering, Rowan University, Glassboro, NJ, USA

Sankaran Mahadevan
Professor, Department of Civil and Environmental Engineering, Vanderbilt University, Nashville, TN, USA

ABSTRACT: A model-based approach for process design and control is more efficient and economical than the physical experiment-based trial-and-error approach in advanced manufacturing processes such as additive manufacturing (AM). However, while employing predictive models it is necessary to take into account the various sources of uncertainty in the computational models in addition to the variability in the AM process. This work presents a Bayesian methodology for building a probabilistic digital twin that integrates physics-based modeling and experimental data, which is then deployed for process design and layer-wise process control in AM. The methodology consists of three steps: model development, initial optimization of process parameters, and adjustment of process parameters during manufacturing. First, a finite element analysis (FEA) model is used to predict porosity in a laser powder bed fusion (LPBF) AM process. Since the FEA model is expensive, a faster surrogate model is constructed to replace the original prediction model and is used for process optimization and control. Data is acquired from in-situ monitoring (e.g., thermal camera) during manufacturing and ex-situ measurement (e.g., X-ray computed tomography) after manufacturing. The error between the model prediction and the observation is calibrated using the measurement data. Based on the corrected prediction model and offline measurement data, the value of the initial process parameters to start the manufacturing process is determined. A robustness-based design optimization method is used to optimize the initial process parameter values while accounting for uncertainty. During manufacturing, the quality of the partially manufactured part is estimated based on the online process monitoring data. Since porosity is not directly observable during the printing process, the temperature profile obtained from the monitoring (using an infrared thermal camera) is used to infer the porosity in the partially finished part. The porosity inference model is constructed by first reducing the dimension of the thermal images by employing singular value decomposition. The prediction model is also updated at every layer based on the monitoring data, and the updated model is used to predict the porosity in the completed part. The predicted porosity is compared to the desired porosity and a decision is made whether the manufacturing should be terminated, continued as-is, or continued with modified process parameters. The effectiveness of the proposed method is demonstrated for controlling process parameters such as laser power and laser speed.

1. INTRODUCTION

Additive Manufacturing (AM), also known as 3D printing, is a process of manufacturing parts by building up layers of material. AM has several advantages over traditional manufacturing methods, including faster prototyping, manufacturing parts with complicated shapes and reducing material waste. Despite the many benefits of AM, inconsistency in the quality of additively manufactured parts has been a major obstacle in the widespread acceptance of AM in the industry. The quality of an AM product is influenced by various factors such as process parameters, print conditions, quality of raw material, etc. The process parameters are controllable parameters and their effect on quantity of interest (QoI) such as geometric accuracy, porosity, residual stress, and fatigue performance have been studied extensively (Oliveira et al. 2020). Since optimizing process parameters using the trial-and-error approach with experimental data is expensive, physics-based model approach for optimizing the process parameters has gained traction (Wei et al. 2021).

Model-based approach in AM introduces several sources of uncertainty to an inherently variable process. AM process have different sources of uncertainties: (a) due to inherent variability in the process (*aleatory uncertainty*) such as powder particle size and laser power/velocity fluctuations, and (b) due lack of knowledge (*epistemic uncertainty*) about the model (uncertain model parameters, errors in the modeling process, and approximation errors) and data (imprecise, sparse, etc.) (Hu and Mahadevan 2017). The various sources of uncertainty contribute to the uncertainty of the predicted QoI (Nath et al. 2019). The uncertainty in variables that make significantly impact the QoI need to be reduced (when possible) and the remaining uncertainty has to be considered in the design optimization process. A few studies have considered uncertainty during process optimization (Nath et al. 2020; Wei et al. 2021). These studies use data collected before the manufacturing starts and thus may not consider the most updated information about the printing system.

Studies have shown that malfunctions in the printer during printing (Megahed et al. 2019) such as change in ambient conditions and degradation of the printer due to lack of maintenance are reflected in the monitoring data collected during manufacturing (Reutzel and Nassar 2015). Thus, it is essential to use real-time monitoring data to detect these malfunctions and change the print conditions to improve the part quality. Previous researchers have investigated feedback process control (Wang et al. 2018) and rapid qualification framework (Megahed et al. 2019); however these studies do not focus on improvement of the quality of the part during printing.

This work seeks to integrate the various elements of online process control discussed above such as model-based prediction of QoI, process monitoring techniques, and uncertainty quantification in AM, to develop a methodology for model-based optimization and control under uncertainty. In the proposed methodology, a physics-based prediction model is first used to estimate the QoI porosity, which is then replaced by a cheaper surrogate model for computational efficiency. Model prediction is then corrected by calibrating a model discrepancy term using offline data. The corrected model is then used for process optimization to determine the initial process parameters to start the manufacturing process. An indirect monitoring strategy is developed to estimate not directly observable porosity from measured temperature data, which also addresses the challenge of high-dimensional data. The prediction model is updated with online monitoring data. The improved model is then used to make decisions about the printing process and to determine updated process parameters, when necessary. The rest of the paper provides the details on the proposed methodology, demonstrates the methodology with an example, and provides concluding remarks.

2. METHODOLOGY

In this section the methodology for model-based process optimization and control under uncertainty is developed by integrating physics-based modeling and experimental data. This methodology is developed with a focus on optimizing and controlling porosity in the selective laser melting (SLM) process of AM. However, the proposed method is generic and is applicable to different processes with corresponding computational models and experimental data. The three main steps in the methodology are (a) model development, (b) initial optimization of process parameters, and (c) adjustment of process parameters during manufacturing. Each step is discussed in detail in the following subsections.

2.1. Model Development

Selective laser melting technique of AM is a process that uses a laser to melt and fuse metal powder particles together, layer upon layer, to manufacture the part. One of the major challenges in producing parts using SLM is controlling and minimizing porosity. Reducing porosity in the component is crucial for obtaining parts with better mechanical characteristics. Porosity in parts can be caused by three factors: insufficient heat leading to unmelted powder (lack-of-fusion porosity), high energy density causing the conversion from conduction mode to keyhole mode processing (keyhole porosity), and trapped gas in the powder during manufacturing (gas porosity). This study focuses on controlling porosity through optimizing SLM process parameters and takes into account lack-of-fusion and keyhole porosity.

2.1.1. Physics-based model

The estimation of porosity in the component is performed through a heat transfer analysis. The governing equation of heat transfer analysis is given by

$$\frac{\partial(\rho C_p T)}{\partial t} = \nabla \cdot k_c \nabla T + Q_h \tag{1}$$

where $\rho, C_p, k_c, T, t, \mathrm{Q_h}$ are density, specific heat, thermal conductivity, temperature, time, and the internal heat generated, respectively. Convection and radiation boundary conditions are applied at the external surfaces.

Thermal history of the part is determined through a finite element (FE) analysis over the entire spatial and temporal domain. The highest temperature at each node (T_i^{max}) is recorded and compared to the material's melting temperature (T_{melt}) and boiling temperature (T_{boil}). If the highest temperature is below the melting temperature, there is a lack-of-fusion porosity. If the highest temperature is above the boiling temperature, there is potential for keyhole porosity. The optimally fused volume fraction (v_{of}) of the part is calculated as the number of nodes with temperatures between the melting temperature and boiling temperature divided by the total number of nodes (N_F) as shown in Eqs. (2) & (3). The goal is to control this fraction, a measure of porosity, to produce a high-quality part.

$$I_i = \begin{cases} 1, & if\ T_{melt} \le T_i^{max} \le T_{boil} \\ & 0, otherwise \end{cases} \tag{2}$$

$$v_{of} = \frac{\sum_i^{N_F} I_i}{N_F} \tag{3}$$

2.1.2. Uncertainty Quantification

As discussed earlier, AM process have different sources of uncertainties (Nath et al. 2019). It is essential to take these uncertainties into account and account for their effect on model prediction. In this work, the difference between the model prediction and actual system behavior is estimated by quantifying the model discrepancy term using experimental data. Model discrepancy term accounts for the assumptions and approximations in the modeling of the complicated AM processes and improves prediction accuracy. However, uncertainty quantification and optimization of process parameters running the model multiple time. Depending on the complexity of the model and available computational resources, using the physics-based model maybe inefficient. Thus, a surrogate model is first constructed to replace the expensive physics-based model. The surrogate model prediction is then corrected by adding a discrepancy term calibrated with experimental data.

2.1.3. Surrogate modeling

Various surrogate modeling techniques can be employed, such as polynomial chaos expansion, artificial neural networks, Gaussian process, decision trees, support vector regression, etc. In this paper, a Gaussian process (GP) model is used (Rasmussen and Williams 2006). The physics-based model $g(\boldsymbol{X})$ with inputs $\boldsymbol{X}$ is replaced with an inexpensive GP model $\hat{g}(\boldsymbol{X})$

$$\hat{\mathrm{g}}(\mathbf{X}) = \boldsymbol{\alpha}(\mathbf{X})^{\mathrm{T}}\boldsymbol{\beta} + \gamma(\mathbf{X}) \tag{4}$$

where $\boldsymbol{\alpha}(\boldsymbol{X})$ and $\boldsymbol{\beta}$ are the trend functions and trend coefficients respectively; $\gamma(\boldsymbol{X})$ is a zero mean Gaussian process with covariance $Cov[\gamma(\boldsymbol{X}_i),\ \gamma(\boldsymbol{X}_j)] = \sigma_\gamma^2 K(\boldsymbol{X}_i,\ \boldsymbol{X}_j)$ for process variance σ_γ^2 and correlation function $K(\boldsymbol{X}_i,\ \boldsymbol{X}_j)$; and $\boldsymbol{X} = [\boldsymbol{X^M}, \boldsymbol{X^P}]$ with $\boldsymbol{X^M}$ and $\boldsymbol{X^P}$ known/unknown model parameters (material properties, etc.) and controllable process parameters (laser power, laser velocity, etc.) respectively.

The accuracy of the surrogate model prediction may be quantified by evaluating the error metrics such as mean absolute error, mean absolute percentage error, mean square error, root mean square error, etc. In this work, mean absolute percentage error (MAPE) is used. The surrogate model error can be improved by using adaptive surrogate model training approaches.

2.1.4. Model discrepancy quantification

The surrogate model is trained with data from the physics-based model corrected for solution approximation errors. Surrogate model is quantified using test dataset (data not used for training the surrogate model) by comparing the surrogate model prediction with physics-based model data. The assumptions and simplifications in the physics-based model causes discrepancy between the model prediction and experimental observation. This model inadequacy is accounted for by using a model discrepancy term δ. Note that when the errors are not quantified individually, the model discrepancy term also includes the contribution of the solution approximation errors, surrogate model error, etc. The relationship between model prediction $\boldsymbol{y_g}$ and experimental data $\boldsymbol{y}_{\text{exp}}$ is given by

$$\boldsymbol{y}_{\text{exp}} = \boldsymbol{y_g} + \delta - \epsilon_{exp} \tag{5}$$

where ϵ_{exp} is the observation error generally represented as $N\left(0, \sigma_{exp}^2\right)$. The formulation of model discrepancy term depends on the problem and availability of data. Using the Kennedy O'Hagan (KOH) framework (Kennedy and O'Hagan 2001), the unknown variables such as unknown model parameters $\boldsymbol{X}^{Mu}$, the parameters of the discrepancy term $\boldsymbol{\theta}_{dis}$, and σ_{exp} are calibrated together.

$$f\left(\boldsymbol{\Theta}\middle|y_{exp}\right) = \frac{f(\boldsymbol{y_{exp}}|\boldsymbol{\Theta})f(\boldsymbol{\Theta})}{\int f\left(\boldsymbol{y_{exp}}\middle|\Theta\right)f(\boldsymbol{\Theta})d\boldsymbol{\Theta}} \tag{6}$$

where $\boldsymbol{\Theta} = \left[\boldsymbol{X}^{Mu}, \boldsymbol{\theta}_{dis}, \sigma_{exp}\right]$; $f(\boldsymbol{\Theta}), f\left(\boldsymbol{y_{exp}}|\boldsymbol{\Theta}\right)$, and $\mathrm{f}\left(\boldsymbol{\Theta}\middle|y_{exp}\right)$ are the joint probability density function (PDF) of $\boldsymbol{\Theta}$, the likelihood function, and the joint posterior PDF. The posterior distribution function is estimated using sampling techniques such as Markov chain Monte Carlo (MCMC) and Sequential Monte Carlo (SMC).

2.2. Process Optimization

Process optimization in AM refers to optimizing the quality or performance of the part such as minimizing defects in the part or maximizing mechanical strength of the part. The manufacturing process starts with optimal process parameters determined using the physics-based simulation model and the existing knowledge about the system. If the process deviates from its expected behavior during the manufacturing process, then process control is implemented.

For a part with $\mathrm{n_l}$ number layer of layers and design variables $\boldsymbol{X_d}$ ($\boldsymbol{X_d} \subseteq \boldsymbol{X^P}$) as inputs, a surrogate model $\Upsilon_F(\mathbf{X_d})$ (Sec. 2.1.3) is first trained using data from the physics model simulations (Sec. 2.1.1) to predict the QoI for a layer. Using offline experimental data y_{D_Υ}, model discrepancy term δ_Υ is calibrated (Sec. 2.1.4) and added to the surrogate model. The objective function $f(\boldsymbol{X_d})$ is given by

$$f(\boldsymbol{X_d}) = \sum_{i=1}^{n_l} \Upsilon_{Fi}(\boldsymbol{X_d}) + \delta_\Upsilon \tag{7}$$

As discussed earlier, AM process and the predictive models have several sources of uncertainties, leading to uncertainty in the model prediction for the quantity of interest. The objective function and the constraints may not be deterministic. Two formulations can be used for optimization under uncertainty: (a) reliability-based design optimization (RBDO) (Zaman and Mahadevan 2017) and (b) robust design optimization (RDO) (Zaman et al. 2011). The RBDO formulation optimizes the objective function by ensuring the reliability of the performance criteria falls below a specified failure probability, while satisfying other design constraints. Estimating the constraint violation probability is challenging in this approach, as it would require many function evaluations given that the failure probability of most systems is very low. In contrast, the RDO formulation focuses on optimizing the objective function while reducing the variance in system performance and adhering to specified bounds for other design constraints. In this work, RDO approach is used as it requires fewer function evaluations and thus is better suited for process control in real-time.

RDO can be framed as a multi-objective optimization problem with two objectives: (a) optimize the mean value of the QoI, and (b) minimize the variance in the QoI. Combining the two objectives using a weighted sum approach, the RDO formulation can be written as

$$\begin{aligned}
& min\, f(\mathbf{X}_d) = \left(w_1 \mu_f(\mathbf{X}_d) + w_2 \sigma_f(\mathbf{X}_d)\right) \\
& s.t. \\
& lb_{g_i} + k_c \sigma_{gi}\big(g_i(\theta_d)\big) \leq g_i(\mathbf{X}_d) \\
& \qquad \leq ub_{g_i} - k_c g_i\big(g_i(\mathbf{X}_d)\big), \\
& \qquad i = \{1, \dots, n_g\} \\
& lb_{\mathrm{X}_{dj}} \leq \mathrm{X}_{dj} \leq ub_{\mathrm{X}_{dj}}, j = \{1, \dots, n_d\} \\
& w_1 + w_2 = 1
\end{aligned} \tag{8}$$

where $\mathbf{X}_{dj}$ is the j-th design variable, $g_i(\mathbf{X}_d)$ is the j-th constraint; n_d and n_g are the number of design variables and constraints, respectively; lb_{g_i} and ub_{g_i} are the lower and upper bounds of g_i, $lb_{\mathrm{X}_{dj}}$ and $ub_{\mathrm{X}_{dj}}$ are the lower and upper bounds of X_{dj}. The robustness in the design constraints in the presence of uncertainty is satisfied by ensuring that the constraints are within the specified bounds of $k_c\sigma_g$, where k_c is a user-defined constant depending on the application and σ_{gi} is the standard deviation of the constraint g_i. The weights w_1 and w_2 denote the relative importance of the objectives. Since the objective function needs to be evaluated multiple times, the surrogate model constructed earlier is used for faster computation. Depending on the number of design variables and the feasible space size, a suitable optimization technique such as brute-force optimization, genetic algorithm, simulated annealing, grid search, trajectory methods, etc. can be used to approximate the optimal solution $\boldsymbol{X}_{opt}$ of Eq. (6). In the example discussed in Sec. 4, exhaustive search technique is used due small feasible space for two design variables. The initial process parameter setting for manufacturing process is the optimal solution $\boldsymbol{X}_{opt}$.

2.3. Online Process Control

Under normal manufacturing environment and conditions, the manufacturing process is expected to produce good quality parts. On the other hand, in case any anomalies occur, the manufacturing process may need to be changed to achieve the desired quality level. Thus, the parts need to be monitored during manufacturing to detect the anomaly, predict the quality of the part from partially manufactured part, and change the process parameters, if necessary, to improve the quality of the part.

2.3.1. Online Monitoring

An efficient monitoring system for online process design and control needs to be in-situ, non-contact, and non-destructive. This poses a challenge when the QoI such as porosity is not directly observable during manufacturing. In such cases, an indirect measurement technique can be employed. A relationship or function (g_q) can be established between an observable quantity (y_{me}) to estimate the QoI that is not directly observable (y_D). For example, thermal images or optical images may be used to estimate porosity.

$$y_D = g_q(y_{me}) \tag{9}$$

Constructing a surrogate model for the function (g_q) in Eq. (7) is not trivial when the input is high-dimensional image data. First, the high-dimensional response input needs to be converted to a low-dimensional latent space. In this work, singular value decomposition (SVD) (Chatterjee 2000) method is used. Then, SVD-based GP surrogate model is constructed.

The spatio-temporal data for different realizations of the process parameters can be written as

$$\boldsymbol{D} = \begin{bmatrix} m(\boldsymbol{v}_1, \boldsymbol{X}_{d1}) & m(\boldsymbol{v}_1, \boldsymbol{X}_{d2}) & \cdots & m(\boldsymbol{v}_1, \boldsymbol{X}_{dn_2}) \\ m(\boldsymbol{v}_2, \boldsymbol{X}_{d1}) & m(\boldsymbol{v}_2, \boldsymbol{X}_{d2}) & \cdots & m(\boldsymbol{v}_2, \boldsymbol{X}_{dn_2}) \\ \vdots & \vdots & \ddots & \vdots \\ m(\boldsymbol{v}_{n_1}, \boldsymbol{X}_{d1}) & m(\boldsymbol{v}_{n_1}, \boldsymbol{X}_{d2}) & \cdots & m(\boldsymbol{v}_{n_1}, \boldsymbol{X}_{dn_2}) \end{bmatrix}^T \tag{10}$$

where $\boldsymbol{v}_1, \boldsymbol{v}_2, \ldots, \boldsymbol{v}_{n_1}$ are the n_1 spatial locations and $\boldsymbol{X}_{d1}, \boldsymbol{X}_{d2}, \ldots, \boldsymbol{X}_{dn_2}$ are the n_2 different realizations in the design domain. The data matrix $\boldsymbol{D}$ is decomposed using SVD as $\boldsymbol{D} = \boldsymbol{PQR}^T$ where $\boldsymbol{P}$ and $\boldsymbol{R}$ are orthogonal matrices, $\boldsymbol{Q}$ is a rectangular diagonal matrix. The diagonal elements $\boldsymbol{\lambda}$ of $\boldsymbol{Q}$, $\boldsymbol{\lambda} = [\lambda_1, \lambda_2, \cdots, \lambda_r]$, $r = min(n_1, n_2)$ are called singular values. Defining $\boldsymbol{\Omega} = \boldsymbol{PQ}$, the original data matrix $\boldsymbol{D}$ can be reconstructed as $\widetilde{\boldsymbol{D}}$ with the first q_s given by

$$D(\boldsymbol{v}_m, \boldsymbol{X}_{di}) \approx \widetilde{D}(\boldsymbol{v}_m, \boldsymbol{X}_{di}) = \sum_{p=1}^{q_s} \Omega_p(\boldsymbol{X}_{di})\, R_p(\boldsymbol{v}_m), \forall i = 1,\ 2,\ \cdots,\ n_2;\ m = 1,\ 2,\ \cdots, n_1 \tag{11}$$

Thus, the high dimensional data matrix $\boldsymbol{D}$ is mapped to low-dimensional latent response Ω_p, $p = 1,2,\cdots, q_s$. SVD-based GP surrogate model ψ_F is constructed with Ω_p as input and $\mathrm{y_D}$ as output. Equation (8) can be written as

$$y_D = \psi_F\,(\Omega_p) \tag{12}$$

2.3.2. Online Control Implementation

The manufacturing process starts with the initial process parameters set at $\boldsymbol{X}_{opt}$, determined using a prediction model corrected with offline data, i.e., data collected before the manufacturing process started. Online process control is based on real-time monitoring data, i.e., data collecting during manufacturing. The monitoring data is used to update the model after every layer considering the process can be controlled by changing the process parameters every layer. The model discrepancy term is calibrated with new observation data at every layer. This updated model is used to find the optimal process parameters for the future layers.

For a partially finished part with n_p number of layers printed, the QoI of the finished part is estimated as

$$q = \sum_{i=1}^{n_p} y_{D_i} + \sum_{i=n_p+1}^{n_l} Y_F\left(\boldsymbol{X}_{\boldsymbol{d_p}}\right) + \delta_{Y_p} \tag{13}$$

where y_{D_i} as the observed QoI after i-th layer is printed, and $\mathbf{X}_{\boldsymbol{d_p}}$ and δ_{Y_p} are the process parameters and model discrepancy term based on data collected from $n_p - th$ layer.

The manufacturing process is controlled by using predictions about the quality of the finished part (QoI) to make decisions on adjusting process parameters. If the predicted quality q is close to the target v_{min}, the process will continue as is. But if it is significantly worse ($q << v_{min}$), the manufacturing will be stopped as the poor quality cannot be fixed by just changing the parameters. If the predicted quality is within a specific tolerance from the target ($v_{min} - \epsilon_d \leq q \leq v_{min} + \epsilon_d$), the part can be improved by adjusting the parameters for future layers.

3. EXAMPLE

The methodology presented in Sec. 2 is illustrated in this section. A part of size 2mm x 0.5mm x 0.18mm is manufactured on a substrate of 4mm x 1.05mm x 0.4mm. The part is built in six layers, each with a thickness of 30µm, using the SLM process. Material properties for Ti6Al4V (Fu and Guo 2014) are considered in this work. Predictive process control is used to maximize the optimally fused volume fraction (v_{of}) by adjusting the laser power (P_L) and laser velocity (V_L).

3.1. Porosity prediction model

The governing equation (Eq. (1)) is first solved using a finite element (FE) method. In the commercial software, Abaqus, variable mesh size is used to improve accuracy: finer mesh for the powder, and coarser mesh for the substrate. The powder layers are simulated using element activation/deactivation technique and the moving heat source is modeled as a Gaussian heat flux with a DFLUX subroutine. The total number of nodes in the powder layers is 53,382 (N_F). The temperature history of the nodes is extracted and using Eqs. (2) & (3), the optimal volume fraction is estimated. On an Intel Core i7-6700 CPU 3.4 GHz, 16GB RAM desktop machine, the computation time is ≈ 9.5 hours with 4 CPUs for the FE analysis including the computational effort for nodal temperature data extraction from output database file.

The expensive FE model is replaced by a cheaper surrogate model to make online process control computationally feasible. Employing design of experiments (DoE), 81 samples of process parameters $\boldsymbol{X_d} = [P_L, V_L]$ are generated and the corresponding value of v_{of} is estimated using the FE model (Figure 1). Then, this dataset is used to train a GP surrogate model. Since the estimated surrogate model error is 1.95%, the surrogate model is accepted for offline process control.

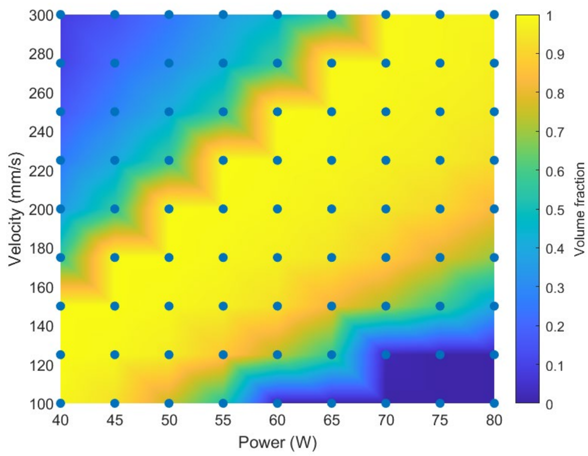

Figure 1: Porosity volume fractions at the DoE sample points

3.2. Offline Process Design

The surrogate model is first used to calibrate the model discrepancy term. In the absence of experimental data, synthetic data is used (generated by adding Gaussian noise N~(0,0.3) to FE model predictions). Then, the surrogate model corrected with calibrated model discrepancy term (Figure 2) is used to determine the optimal process parameters. The optimal solution for the RDO formulation with $w_1 = 1, w_2 = 0$ is $\boldsymbol{X}_{opt} =$ [76,203] is the initial parameter setting.

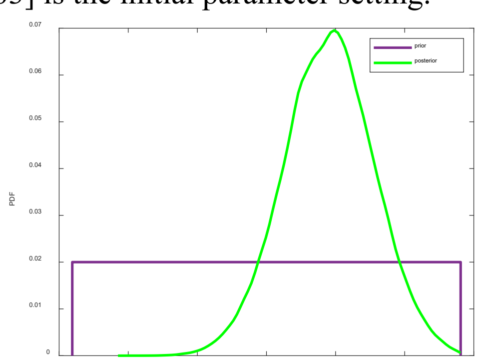

Figure 2: Calibration of model discrepancy term

3.3. Online Process Monitoring and Control

Porosity is not directly observable; thus a surrogate model needs to be constructed as discussed in Sec. 2.3.1. In this example, it is considered that temperature data from thermal images are used to estimate porosity (v_{of}). Since MAPE value of reconstruction with first 6 important features is 0.44%, surrogate model for porosity estimation is created with the first 6 important features. This surrogate model with MAPE value of 0.87% is used for process control.

Assuming the target porosity $v_{min} = 0.9$, and $\epsilon_d = 0.2$; part is acceptable if $v_{of} \geq v_{min}$. If a part has $v_{of} < (v_{min} - \epsilon_d)$, manufacturing is terminated as it is assumed that there is serious anomaly in the printing system. When $v_{min} \leq v_{of} \leq (v_{min} - \epsilon_d)$, process control is implemented. To illustrate the process control methodology, an anomaly is simulated by considering the process parameters realized by the printer is $P_C = 0.95\, P_L$, $V_C = 0.9 V_L$. Layer-wise process control is implemented by considering this anomaly and starting the manufacturing process at $\boldsymbol{X}_{opt} = [76, 203]$. Figure 3 shows that in a printing system where an anomaly is present, implementing process control procedure produces part with acceptable quality. Whereas if the process is continued as-is the part produced is of poor quality.

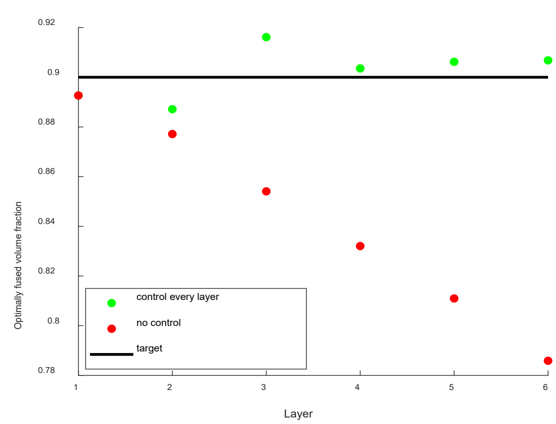

Figure 3: Comparison between controlled and no-control processes

The process parameters (P in W, Velocity in mm/s) for the controlled procedure are: [(76, 203), (69,182), (62,167), (62,146),(57,148),(62,156)].

Similar to Sec. 3.2, synthetic data is used as experimental data is not available. The computational effort necessary to implement process control for each layer is ≈55 seconds.

4. CONCLUSIONS

This paper proposes a methodology for model-based optimization and control under uncertainty. The three main components of the proposed methodology: model development, offline process design, and online process control. For computational efficiency during uncertainty analysis and optimization, surrogate modeling and dimension reduction technique have been employed. The method is demonstrated on layer-wise predictive process control of porosity in an SLM AM. When process control is implemented, the finished part has better quality in comparison to uncontrolled process. In the future, this methodology may be improved by validating with experimental data and using sophisticated, more accurate physics-based model. Fast collection and analysis of monitoring data and the time lag between printing of two layers when control is implemented also needs to be studied.

5. REFERENCES

Chatterjee, A. (2000). "An introduction to the proper orthogonal decomposition." *Current science*, 808-817.

Fu, C., and Guo, Y. "3-dimensional finite element modeling of selective laser melting Ti-6Al-4V alloy." *Proc., 2014 International Solid Freeform Fabrication Symposium*, University of Texas at Austin.

Hu, Z., and Mahadevan, S. (2017). "Uncertainty quantification and management in additive manufacturing: current status, needs, and opportunities." *The International Journal of Advanced Manufacturing Technology*, 93, 2855-2874.

Kennedy, M. C., and O'Hagan, A. (2001). "Bayesian calibration of computer models." *Journal of the Royal Statistical Society: Series B (Statistical Methodology)*, 63(3), 425-464.

Megahed, M., Mindt, H.-W., Willems, J., Dionne, P., Jacquemetton, L., Craig, J., Ranade, P., and Peralta, A. (2019). "LPBF right the first time—The right mix between modeling and experiments." *Integrating Materials and Manufacturing Innovation*, 8(2), 194-216.

Nath, P., Hu, Z., and Mahadevan, S. (2019). "Uncertainty quantification of grain morphology in laser direct metal deposition." *Modelling and Simulation in Materials Science and Engineering*, 27(4), 044003.

Nath, P., Olson, J. D., Mahadevan, S., and Lee, Y.-T. T. (2020). "Optimization of fused filament fabrication process parameters under uncertainty to maximize part geometry accuracy." *Additive manufacturing*, 35, 101331.

Oliveira, J. P., LaLonde, A., and Ma, J. (2020). "Processing parameters in laser powder bed fusion metal additive manufacturing." *Materials & Design*, 193, 108762.

Rasmussen, C. E., and Williams, C. K. (2006). *Gaussian processes for machine learning*, Springer.

Reutzel, E. W., and Nassar, A. R. (2015). "A survey of sensing and control systems for machine and process monitoring of directed-energy, metal-based additive manufacturing." *Rapid Prototyping Journal*, 21(2), 159-167.

Wang, Q., Li, J., Nassar, A. R., Reutzel, E. W., and Mitchell, W. "Build height control in directed energy deposition using a model-based feed-forward controller." *Proc., Dynamic Systems and Control Conference*, American Society of Mechanical Engineers, V002T023A003.

Wei, H., Mukherjee, T., Zhang, W., Zuback, J., Knapp, G., De, A., and DebRoy, T. (2021). "Mechanistic models for additive manufacturing of metallic components." *Progress in Materials Science*, 116, 100703.

Zaman, K., and Mahadevan, S. (2017). "Reliability-based design optimization of multidisciplinary system under aleatory and epistemic uncertainty." *Structural and Multidisciplinary Optimization*, 55, 681-699.

Zaman, K., McDonald, M., Mahadevan, S., and Green, L. (2011). "Robustness-based design optimization under data uncertainty." *Structural and Multidisciplinary Optimization*, 44, 183-197.